

Accurate Particles Characterization in Lipid Nanoparticle Therapies

Waters Corporation, United States

Published on November 06, 2025

Introduction

Lipid nanoparticles (LNPs) have emerged as one of the most promising drug delivery methods¹. LNPs encapsulate genetic material in submicrometer sized lipid vesicles, deliver large biologic payloads, exhibit low immunogenicity, and can enable large manufacturing scalability as seen with the Moderna® and Pfizer® mRNA COVID-19 vaccines. Like all biologics, LNPs can be physically unstable², aggregate, and form subvisible particles (SVPs), and thus need to be properly formulated and evaluated for physical and chemical stability³. The next generation of LNPs are even more chemically and biologically complex than their predecessors¹, presenting unique challenges in both their stability and manufacturability. Accurate low volume subvisible particle measurements will form a critical aspect of the quality assessment of LNPs.

Like all injectables, LNPs are subject to USP 787/788 SVP testing⁴. However, USP 788 compendial Method 1, light obscuration (LO), is deemed “unsuitable to measure liposomal and colloidal suspensions” as stated in the chapter. In fact, USP 788 recommends membrane microscopy (Compendial Method 2) for measuring liposomal formulations, given LO’s inability to handle solutions with a complex matrix⁴. Aura® uses Backgrounded Membrane Imaging (BMI), a form of membrane microscopy that enables high throughput, low volume subvisible particle characterization.

In this application note, we demonstrate how Aura GT can accurately and thoroughly characterize the subvisible

particle content of LNPs with volumes as little as 25 μ L per sample. We focus on the analysis of two LNP samples formulated in different buffers and subjected temperature and freeze thaw stresses. In addition, we use Aura GT's SYBR™ Gold assay⁵ to help characterize nucleic acid escape in stressed LNP samples and quantitatively analyze the stability and purity of these samples.

Experimental

Sample Composition

Two novel LNPs samples, hereby referred to as Sample A and Sample B, encompass a lipid capsule with RNA payload. The two LNPs are of similar lipid composition as the Moderna COVID-19 vaccine and contain Moderna's ionizable lipids PEG-DMG and SM-102, cholesterol, and distearoylphosphatidylcholine (DSPC), with lipid and RNA concentrations of 0.9 mg/mL LNP, 45 μ g/mL of RNA, respectively. Monomeric diameters were characterized via dynamic light scattering (DLS) with Sample A measuring 110 nm and Sample B measuring 140 nm.

Forced Degradation Study

Sample A and Sample B were subjected to:

- a) Thermal stress: 80 °C heating for 2 hours
- b) Freeze thawing: Both samples were subjected to three rounds of freeze thawing (FT) at -80 °C and 23 °C over a period of 6 hours
- c) Buffers: LNPs were formulated in 3 separate buffers: acetate (50 mM acetate, 150 mM sodium chloride, pH=4.79), PBS and glycine (50 mM glycine, 50 mM NaCl, 100 mM arginine, pH=10.6)

Particle Measurements

LNP samples were measured using BMI and Fluorescence Membrane Microscopy (FMM) using Aura GT on a black membrane plate. This procedure was adapted for each stress condition three wells were loaded with 25 μ L per well, and the filtrate stained with 1x SYBR Gold (2% v/v DMSO in PBS) for 1 min prior to FMM measurements. This procedure was adapted from Application note 16.⁵

Results and Discussion

Figures 1a and 1b show the subvisible particle size distributions for both LNP sample types under no stress, 80 °C and freeze thaw stress. Both samples showed unique subvisible particle size distributions corresponding to their stress conditions. Both Sample A and Sample B exhibited significant subvisible particle counts ($\geq 2 \mu\text{m}$), exceeding $2 \times 10^6/\text{mL}$ for the non-stressed conditions. The greatest impact on particle count was observed with three cycles of FT stress in both sample A and B whereby counts increased by 47% and 25% respectively, when compared to no stress. Under heat stress, Sample A formed larger amounts of small ($\geq 2 \mu\text{m}$) subvisible particles than Sample B, while Sample B formed larger amounts under cold stress. Across all conditions, Sample A formed larger amounts of large subvisible particles ($\geq 10 \mu\text{m}$) than Sample B. Neither sample showed significant large subvisible particles ($\geq 25 \mu\text{m}$) under any stress condition, essential for stable formulation control. Heat stressed samples showed a 5- to 10-fold reduction in subvisible particle formation for both sample types across the entire subvisible range, suggesting LNP particle formation as temperature dependent.

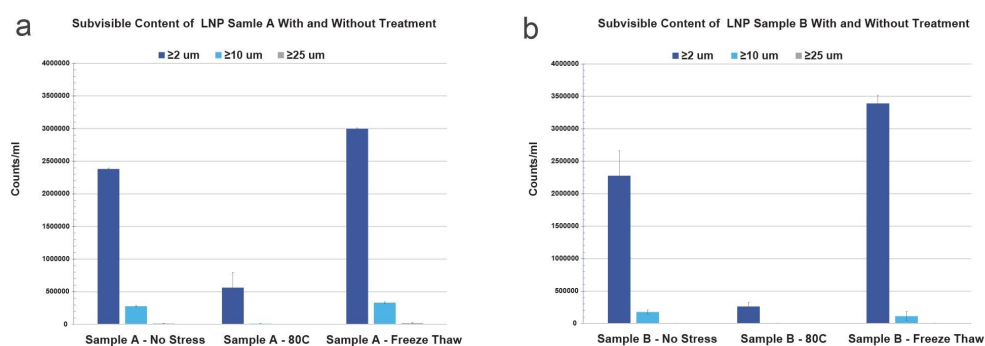


Figure 1. Comparison of SVP size distributions ($\geq 2 \mu\text{m}$, $\geq 10 \mu\text{m}$ and $\geq 25 \mu\text{m}$) of two LNP samples, a) Sample A and b) Sample B as a function of stress condition; no stress, incubated at 80°C for two hours and three cycles of freeze-thaw.

In *Figure 2*, we take a deeper look at the subvisible particle images for Sample A before applying stress and after freeze thawing. The freeze thawed membrane images are shown in three imaging modes (2a) BMI, (2c) SYBR Gold fluorescence and (2e) combined BMI and SYBR Gold fluorescence image, whereas the unstressed sample images are in (2b) BMI, (2d) SYBR Gold fluorescence and (2f) combined BMI and SYBR Gold fluorescence images. Both sets of BMI membrane images show significant subvisible particle formation for unstressed and

stressed types. Upon staining both the unstressed and freeze thawed samples with SYBR Gold, that the stressed sample shows significant area portions of strong SYBR Gold fluorescence, indicating insoluble samples that are coated with nucleic acid material, whereas no fluorescence signal is visible in the unstressed sample.

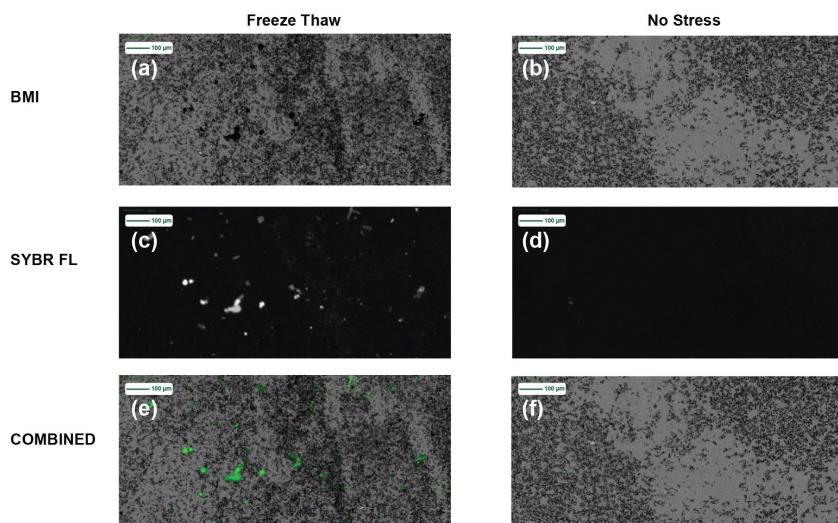


Figure 2. Subvisible particle images of no stress and freeze thawed conditions for Sample A. Blue scale bar is 100 μm long. Freeze thawed condition (a) BMI, (c) SYBR Gold fluorescence, and (e) combined BMI and SYBR Gold images. No stress (b) BMI, (d) SYBR Gold fluorescence, and (f) combined BMI and SYBR Gold fluorescence images.

Figure 3 shows the $>2 \mu\text{m/mL}$ subvisible particle concentrations for Sample A and Sample B formulated in three separate buffers: acetate, glycine and PBS. All particle measurements showed significant particle concentrations ($>1.5\text{E}6/\text{mL}$) across all conditions, with exceptionally good repeatability (CVs $<15\%$). In addition, both samples exhibited subvisible particle formation that did not vary beyond measurement uncertainty with buffer type.

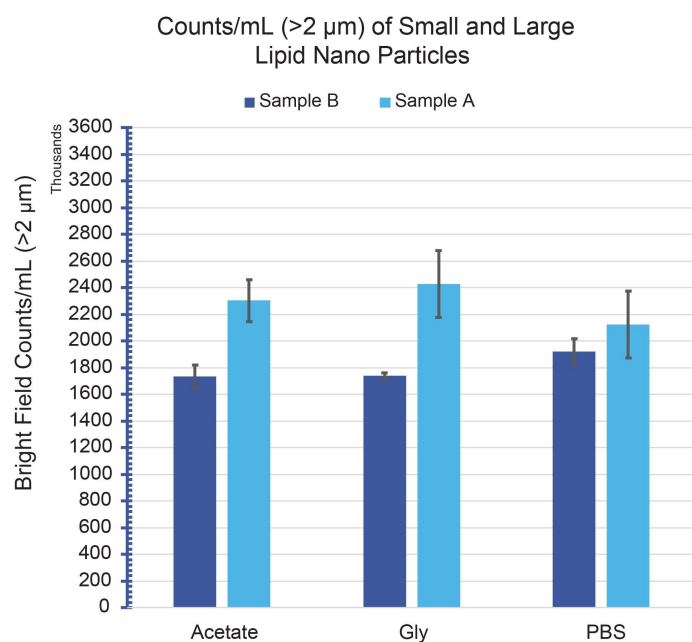


Figure 3. Subvisible particle counts (>2 $\mu\text{m/mL}$) for Sample A and Sample B treated with varying buffers.

Figure 4 shows Sample A (a) Before filtration (b) After 1 round of 0.2 μm filtration (c) After 2 rounds of 0.2 μm filtration. The requirement for two rounds of filtration for SVP clearance is an important observation as it suggests that particle formation can occur post filtration presumably in a concentration dependent manner.

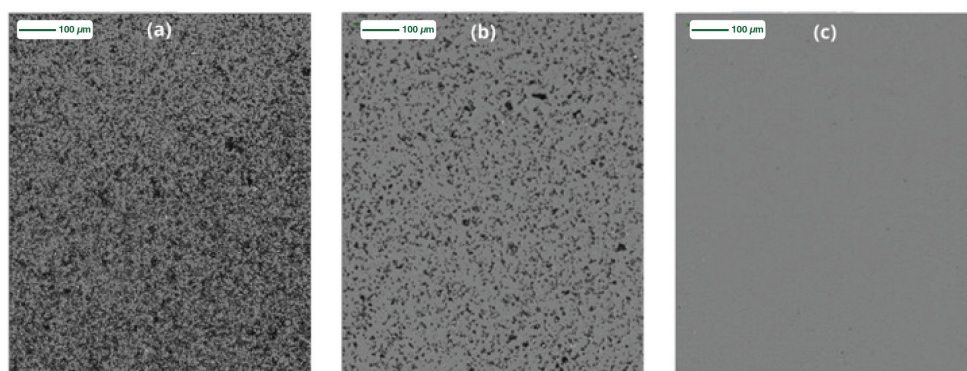


Figure 4. Assessment of LNP particle clearance using filtration. Particle images of Sample A (a) before filtration, (b) after 1 round of 0.2 μm filtration, and (c) after 2 rounds of 0.2 μm filtration

Conclusion

Both samples A and B showed significant subvisible particle formation, more than $1 \times 10^6/\text{mL}$ $>2 \mu\text{m}$ across most conditions except thermal stress, pointing to inherently unstable LNP formulations. Freeze thaw cycles significantly increased subvisible particle formation, while heat stress significantly reduced the subvisible particle concentration across both samples. Compared to protein formulations, this heat stress effect may appear unconventional. However, considering the LNP composition and upon further look at the literature, we are able to understand this phenomenon and conclude that significant heat stress can break a liposomal formulation apart³, increasing the LNP solubility and thereby resulting in less insoluble particles captured on the membrane. On the other hand, freeze thawing produces more insoluble aggregates, thereby increasing subvisible counts as shown in BMI, exhibiting similar behavior to heat induced aggregation as in most protein formulations. A recurring theme in subvisible particle stability is that each formulation exhibits its own particle profile, LNPs are no exception. Another interesting data point is that freeze thawed LNPs showed significant SYBR Gold staining, whereas unstressed LNPs did not, indicating a unique nucleic acid leakage or rupture behavior for this type of stress. Finally, we also observed that buffer type did not significantly impact the subvisible particle count (data not shown). Whilst we observed significant particle counts across all samples tested, pH and buffer variance did not significantly increase particle formation. Indeed, several LNP formulations have reported robust stability

profiles across a variety of buffers³. Filtration of the final product may not be appropriate, as particle formation occurs following filtration, most likely in a concentration dependent manner (Figure 4). Multiple filtration steps, whilst able to clear the product, will undoubtedly result in reduced concentration of pharmacologically active LNPs and as a function of time particles will return as described in our “What Happens When I Filter My Sample” Application Note 21.

In conclusion, Aura enables high throughput, low volume, accurate sub-visible particle analysis with direct applicability for LNP stability assessment. Arcane particle analysers, unsuitable for LNP assessment, will struggle to overcome the challenges associated with the physical and chemical complexity of LNPs. Indeed, Aura resolved these key challenges, providing a solution to sub-visible particle analysis of LNPs, from early stage inception through to product release.

References

1. Xu, L., Wang, X., Liu, Y., Yang, G., Falconer, R.J. and Zhao, C. (2022), Lipid Nanoparticles for Drug Delivery. *Adv. NanoBiomed Res.*, 2: 2100109. <https://doi.org/10.1002/anbr.202100109> <
<https://doi.org/10.1002/anbr.202100109>>
2. Ball RL, Bajaj P, Whitehead KA. Achieving long-term stability of lipid nanoparticles: examining the effect of pH, temperature, and lyophilization. *Int J Nanomedicine*. 2016 Dec 30;12:305-315. doi: [10.2147/IJN.S123062](https://doi.org/10.2147/IJN.S123062) <
<https://pubmed.ncbi.nlm.nih.gov/28115848/>> . PMID: 28115848; PMCID: PMC5221800.
3. Trenkenschuh E, Savšek U, Friess W. Formulation, process, and storage strategies for lyophilizates of lipophilic nanoparticulate systems established based on the two models paliperidone palmitate and solid lipid nanoparticles. *Int J Pharm*. 2021 Sep 5;606:120929. doi: [10.1016/j.ijpharm.2021.120929](https://doi.org/10.1016/j.ijpharm.2021.120929). Epub 2021 Jul 23. PMID: 34303819.

Featured Products

[Aura GT System </nextgen/ch/de/products/particle-analyzers/aura-gt.html>](https://www.nextgen.ch/de/products/particle-analyzers/aura-gt.html)



© 2025 Waters Corporation. All Rights Reserved.

[Nutzungsbedingungen](#) [Datenschutzhinweis](#) [Marken](#) [Karriere](#) [Rechtliche Hinweise](#) und [Datenschutzhinweise](#) [Cookies](#) [Cookie-Einstellungen](#)